

## 3 Radiators

---

### 3.1 General considerations and requirements

Transition radiation (TR) is produced when a highly relativistic charged particle traverses the boundary between two media of different dielectric constants [1]. As the average energy of the emitted TR photon is approximately proportional to the Lorentz factor  $\gamma$  of the particle (for  $\gamma$  around a few thousand), this provides an excellent way for discriminating between electrons and pions for momenta of a few GeV/c and higher. However, the probability of photon emission from a single boundary is very small, so that a large number of boundaries have to be combined to obtain a reasonable efficiency. Commonly used are stacks of a few hundred polypropylene foils which have a regular periodic structure and which in earlier tests have been shown to be the most efficient radiators available [2, 3]. For a general review about transition radiation detectors see [4].

In the environment of the complete ALICE detector the radiator of the TRD, besides providing a high efficiency for transition radiation, has to fulfill geometrical and mechanical constraints. The detector consists of 6 identical layers each of which has full azimuthal coverage. Within these cylinders there has to be as little dead material as possible to avoid acceptance losses. Furthermore the total amount of material shadowing other detectors has to be minimized. Strong metal frames which would be required to mount hundreds of foils are therefore not adequate. Even then, for the size of the radiators foreseen, and taking into account the collider geometry, it would not be possible to maintain a uniform separation of the foils. Already these circumstances exclude the use of foil radiators. In addition, a foil based design would lead to an unacceptable complexity in the construction of the 540 radiators.

The radiator itself is intended to support the front window of the readout chambers which serves simultaneously as the drift electrode. The radiator has to guarantee that a maximum allowed deviation from a flat surface of the window is not exceeded. Slight but non negligible overpressure in the chambers due to gravity and flow of the Xe,CO<sub>2</sub> gas mixture leads to a bending of the window. This bending would lead to non uniform drift times in the chambers due to distortions in the drift field configuration and drift length. Also the radiator should add as much as possible to the total mechanical stability of the chambers.

Two other types of radiator materials have therefore been investigated:

- fibres layered in predominantly two-dimensional mats
- foams with more or less random internal structure.

The fibre mats can be regarded as approximations to foil stacks, as the fibre thickness provides a well defined spatial separation between two consecutive boundaries and a reasonably large fraction of the boundaries is approximately perpendicular to the measured particles, while foams with their irregular structure have both random orientation of the boundaries and variable size spatial gaps between them. It is therefore not surprising that the TR response of fibre radiators is comparable to foils and that foams are slightly less efficient. However, the mechanical properties of foams are far superior to those of fibre mats (see Chapter 14).

Since interactions like multiple scattering, conversion and bremsstrahlung in the used material affect the performance of the TRD itself and of the other ALICE subdetectors positioned behind it, the overall material budget is limited. This sets another restriction to the choice of materials.

The requirements on the TRD radiator can be summarized as follows:

- It has to generate transition radiation with sufficient efficiency while not exceeding the foreseen thickness of 4.8 cm .

- It should provide support to the entrance window and constrain its deflection caused by the gas pressure to below 1 mm .
- The 6 layers of radiator as the most important single contributor should bring the total amount of material of the TRD not significantly above 15% of a radiation length (see Chapter 10).

## 3.2 Radiator design

Various radiator materials and types (foils, foams and fibres) were tested during extensive test measurements at GSI darmstadt (see Chapter 14). From this experience, in conjunction with the requirements explained above, the following radiator design was chosen. We plan to use a sandwich construction of foam and fibres providing the optimal combination of TR efficiency and mechanical stability.

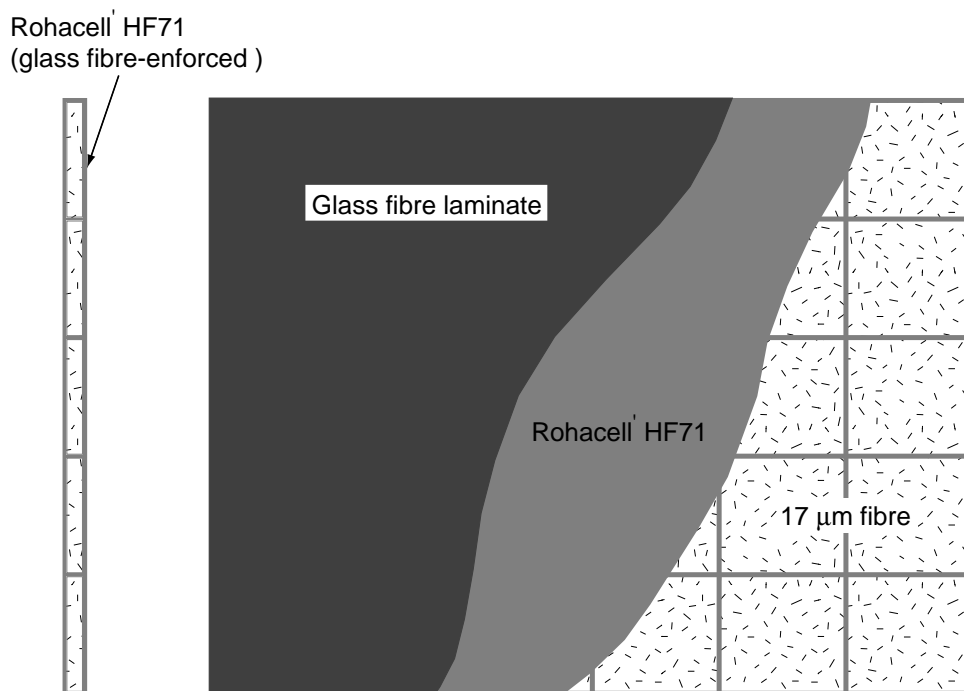


**Figure 3.1:** The principal design of the TRD sandwich radiator.

Fig. 3.1 shows the principal design of the radiator sandwich. The supporting structure is made out of Rohacell *HF71* foam [5]. This material is a PMI (polymethacrylimide) foam with low density and high mechanical and chemical stability. In addition to the supporting function the foam has also a quite good transition radiation production rate (see Chapter 14). The upper and lower covers are made out of Rohacell plates with a thickness of 8 mm reinforced by glass fibre sheets. The glass fibre sheets laminated onto the surface have a thickness of 0.1 mm . The inner side of the radiator will be covered by a 25  $\mu\text{m}$  aluminized Mylar foil which forms the entrance window and the drift electrode of the readout chamber.

The upper and lower covers of the sandwich are connected by a grid-like structure also made out of 8 mm Rohacell. The cell sizes will be adjusted to the dimensions of each radiator. The inner volume of the sandwich cells is filled with polypropylene fibres [6] which serve as the main radiator material (later

on called *fibres17*). Tests have shown that the fibres are comparable in performance to foil radiators (see Chapter 14). Scanning electron microscope pictures of both materials are shown in Fig. 3.2. The properties of the used materials are given in Table 3.1.

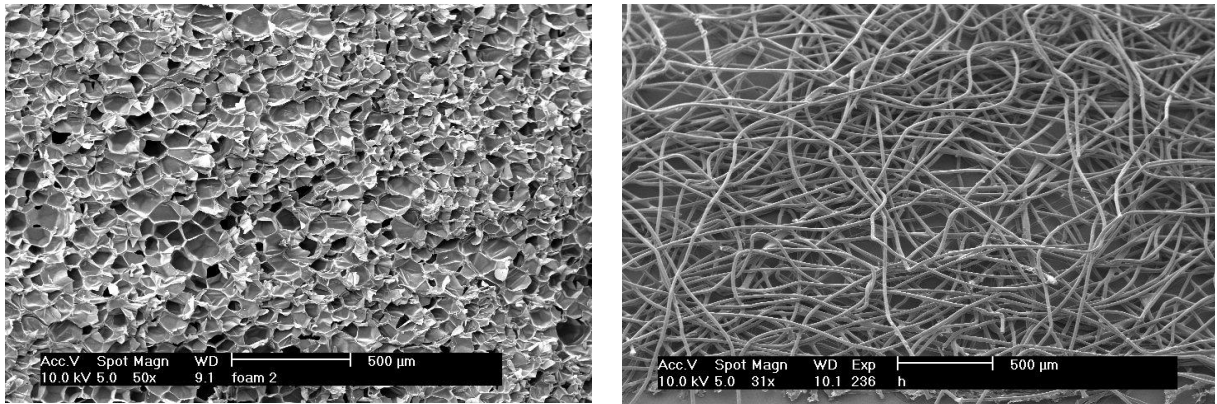


**Figure 3.2:** Scanning electron microscope images of the used radiator materials. Left panel: Rohacell HF71 foam; right panel: fibres mat.

**Table 3.1:** The properties of the compared radiators and their materials. The label *S-HF71* denotes the HF71/fibre sandwich construction.

radiator	material	density [g/cm <sup>3</sup> ]	elastic modulus [MPa]	radiation length $X_0$ [g/cm <sup>2</sup> ]	thickness	
					absolute [cm]	$X/X_0$ [*10 <sup>-3</sup> ]
<i>HF71</i>	Rohacell HF71	0.075	92	40.6	4.8	8.88
<i>fibres17</i>	Polypropylene	0.074	-	44.6	4.0	6.75
<i>S-HF71</i> sandwich	Rohacell HF71	0.075	92	40.6	2*0.8	2.96
	Polypropylene	0.074	-	44.6	3.0	5.30
	sum of materials	-	-	-	4.8	8.26
<i>S-HF71</i> with reinforcement	Glass fibre coating	1.7	> 10 <sup>3</sup>	33.0	2*0.01	1.03
	sum of materials	-	-	-	4.8	9.29

A prototype of a radiator sandwich which covers the largest readout chamber was constructed using Rohacell foam without reinforcement. Its mechanical properties have been measured. Assuming a maximum overpressure of 1 mbar the measured deviation from a flat surface was 3.25 mm. The measurements were done with a uniform areal overpressure simulated by adding water on top of the surface of the horizontally oriented radiator. In addition tests were made with a reinforced radiator model of the dimensions 120 × 20 cm<sup>2</sup>, which corresponds to the full size radiator only in the smaller dimension. The model was supported at the short edges and the deflection measured under load. These tests can be seen as conservative with respect to the full size radiator as the latter would have additional support at the other sides. A reinforcement with carbon fibre rods with a diameter of 2 mm on both sides reduced the deflection below 0.9 mm. In this test setup the reinforcement is approximately equivalent to a carbon fibre laminate of 30 μm thickness on both sides of the radiator sandwich. A photograph of the reinforced radiator model during the tests is shown in Fig. 3.3.

Calculations show that a reinforcement with 100 μm glass fibre on both sides of the sandwich also leads to a deformation of below 0.9 mm for an overpressure of 1 mbar, which meets the requirements.



**Figure 3.3:** The bending test of the reinforced radiator model. One can see the radiator model (white) and the carbon fibre rod (black) glued to it. The overpressure is simulated by weights (in this case screws) distributed over the whole length of the model. The deflection is measured by the dial gauge positioned at the center of the model.

### 3.3 Radiator performance

The transition radiation yield of the sandwich as discussed above and indicated in Fig. 3.1 was measured and compared with similar measurements of the individual materials used in this design. This was done during several test beamtimes at GSI. A mixed beam of electrons and pions was used. For a detailed description of the setup and the measurements refer to Chapter 14.

In the left plot of Fig. 3.4 one can see a typical spectrum of average pulse height vs. drift time for electrons of 1 GeV/c momentum. The signal was measured with an 8-bit flash-ADC system in 60 time bins of 50 ns each. The distribution shows a peak at early times, originating from the amplification region (see Chapter 14). Without transition radiation one would expect a plateau at later times, caused by the energy loss of particles in the drift region. The transition radiation signal sits on top of this plateau and causes a rise of the average signal. This rise is most prominent at later times (around  $2.1 \mu\text{s}$  in this configuration, corresponding to the entrance of the readout chamber) where it builds a second peak in the distribution.

To allow a qualitative comparison of the radiators, the ratio of electron and pion signals are plotted in the right part of Fig. 3.4 as a function of the depth of the chamber, expressed in drift zone number (0 is the amplification region and 4 corresponds to the entrance of the detector). Here the sandwich radiator *S-HF71* is compared with the pure materials *HF71* and *fibres17* for the momentum of 1 GeV/c. Without the contribution of TR one expects a flat distribution at about 1.45 (shaded area in the right panel of Fig. 3.4). At later times (large drift zone number) one can clearly see the effect of the TR, which causes a strong rise of the ratio (about 25 %). This rise is equally pronounced for all three radiators. In this measurement the absolute thickness of the radiator *fibres17* was smaller than that of the two others (40 mm instead of 48 mm). Therefore the electron to pion ratio of this radiator is slightly below the one of the sandwich radiator *S-HF71* at later drift times.

Whereas the ratio of the average signals for electrons and pions is useful for a comparison of different radiator types, for the final estimate of the performance of the detector it is more appropriate to look at

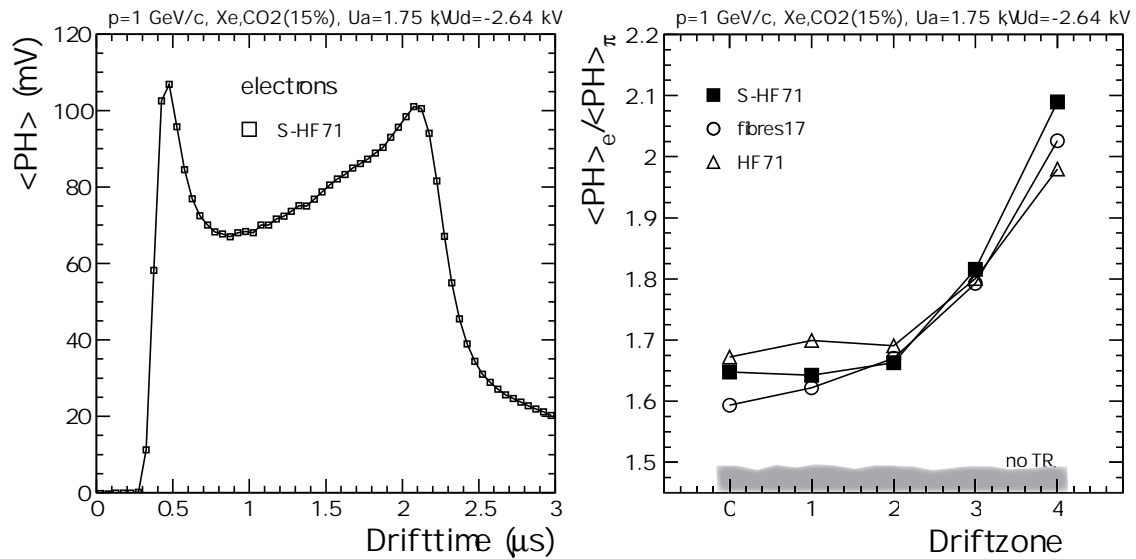


**Figure 3.4:** Left: Average pulse height vs. drift time for 1 GeV/c electrons measured with the sandwich radiator *S-HF71*. Right: Comparison of the different radiator materials (see table 3.1). Shown is the ratio of the mean signals for electrons and pions vs. the drift time for 5 drift zones for 1 GeV/c momentum. The fibre radiator had a smaller thickness of 40 mm compared to 48 mm in case of the other radiators.

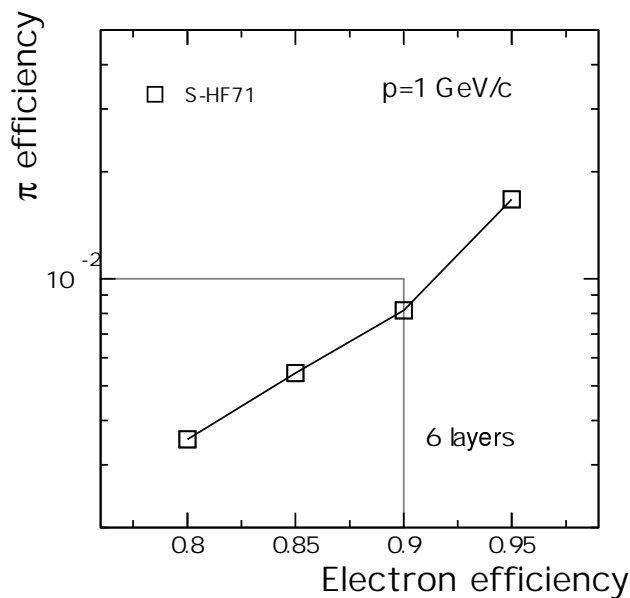


**Figure 3.5:** Pion efficiency as a function of the electron efficiency for the sandwich radiator *S-HF71* extrapolated to 6 layers. The particle momentum was 1 GeV/c and the method of likelihood on integrated charge was used.

the pion rejection performance. In Fig. 3.5 the pion rejection efficiency is plotted as a function of electron efficiency extrapolated to a stack of 6 TRD modules. For this analysis a likelihood method was used, based on the energy deposited in the drift region ( $L-Q$ , see section 14.3.5). The proposed radiator meets the design criteria of a pion rejection of  $10^{-2}$  with an electron efficiency of 90% already at a particle momentum of 1 GeV/c.